The Effect of Waste Loading on Phase Composition, Structure and Chemical Durability of Glassy Materials for Immobilization of High-Sodium/Aluminum Waste - 11475

S.V. Stefanovsky A.S. Sorokaletova, G.A. Malinina
SIA RADON, 7th Rostovskii lane 2/14, Moscow 119121 Russia, profstef@mtu-net.ru

B.S. Nikonov
Institute of Geology of Ore Deposits RAS, Staromonetniy lane 35, Moscow 119117 Russia

ABSTRACT

Mixtures of surrogates of high level waste with high sodium and aluminum contents and sodium-lithium borosilicate frit were placed in alumina crucible, heated to 1200-1300 °C depending on waste to frit ratio in a resistive furnace and kept at melting temperature for 1 hr. Portions of melts were poured onto a metal plate (quenched) and the residues were slowly cooled in turned-off furnace (annealed). The quenched materials contained up to 45 wt.% waste oxides were fully amorphous whereas in the materials with higher waste loadings minor spinel structure phases occurred. The annealed materials with waste loading of up to 45 wt.% contained minor spinel type phase and trace of nepheline $(Na,K)AlSiO_4$. In the annealed materials contained waste oxides in amount of 50 wt.% and more nepheline and spinel were found to be major and minor phases, respectively. Two spinel varieties – first and second generation different in crystal size and geometry occurred. The materials at 55, 60 and 65 wt.% waste loadings are nearly fully crystalline and contain, except nepheline and spinel, extra Cs-bearing phases. These phases co-exist with nepheline and their chemical compositions are recalculated to formulae with 4 oxygen ions. One of them contains up to 0.30 Cs^+ and 0.13 S^{6+} ions per formula, chemical composition of the second one is close to $CsAlSiO_4$. Chemical durability of the materials worsens with waste loading but even at waste loading of 55 wt.% normalized releases of B, Li, Na and Si from the material determined using PCT procedure remain lower than those from EA glass.

INTRODUCTION

Vitrification is the most promising method of consolidation and immobilization of high level waste (HLW). Borosilicate glass is established to be a recommended HLW form in USA, France, UK, Germany, Japan, Korea, India whereas aluminophosphate glass is currently used in Russia [1]. Joule heated ceramic melter (JHCM) is considered as a basic unit in USA, Russia, Germany, Japan, India and inductively heated metallic melter (hot crucible) is used in France. A cold crucible induction melter is believed to be alternative to both JHCM and hot crucible and computation, design and testing works are conducting in France, Russia, USA, India, Korea, and Italy [2-5]. The only in the world a full-scale cold crucible based plant for vitrification of low- and intermediate-level wastes (LILW) is under active operation now in Russia at SIA Radon [3].

Successful demonstration of commercial application of the cold crucible inductive melting (CCIM) technology for treatment of LILW in Russia and feasibility of vitrification of HLW of French [2] and US HLW [4,5] allowed us to propose the CCIM technology for vitrification of some Russian liquid HLW streams currently stored in tanks [6]. Unlike current HLW

vitrification in Russia where aluminophosphate glass is produced, the CCIM technology allows to producing borosilicate and aluminosilicate glasses and glass-crystalline materials. Some results on design, production and examination of glassy forms potentially suitable for long-term storage of Russian HLW are described in the present paper.

Unlike current single-step vitrification technology using liquid feeding of a mixture of high-Na/Al waste and phosphorus acid in a JHCM, the CCIM based technology is suggested to be two-step. The first step is either evaporation/concentration of liquid HLW in a rotary thin-film evaporator following by slurry feeding of concentrate and glass formers as a mixture or separately into cold crucible or direct evaporation/calcinations of waste in calciner following by dry feeding into cold crucible.

EXPERIMENTAL

Specified chemical compositions of high-Na/Al calcine and glassy materials are shown in Table I. The calcine was prepared as follows. Calculated amounts of reagent-grade Na, K, Mg, Ca, Al, Cr, Mn, Fe, and Ni nitrates and Na_2SO_4 were dissolved in a deionized water, the solutions obtained were intermixed with silica, dried and calcined at 600 °C for 5 hrs. The product was ball-milled. Mixtures of synthetic calcine and lithium-sodium-borosilicate frit were put in 50 cc alumina crucibles, placed in a resistive furnace and heated step-by-step to melting temperatures of 1150 °C to 1300 °C depending on mixture composition. Melts were kept for 1 hr at melting temperature followed by pouring of a part of the melt onto a metal plate and cooling of residues in crucibles to room temperature in turned-off furnace.

Table I. Specified chemical compositions (wt.%) of calcine and glasses.

Oxides	Calcine	Glass #							
		1	2	3	4	5	6	7	8
Li_2O	-	5.6	5.2	4.8	4.4	4.0	3.6	3.2	2.8
B_2O_3	-	5.6	5.2	4.8	4.4	4.0	3.6	3.2	2.8
Na_2O	25.9	16.2	16.9	17.6	18.3	19.0	19.6	20.3	21.0
MgO	0.9	0.3	0.3	0.3	0.4	0.4	0.5	0.5	0.6
Al_2O_3	36.5	11.0	12.8	14.6	16.4	18.3	20.1	21.9	23.7
SiO_2	0.0	50.4	46.8	43.2	39.6	36.0	32.4	28.8	25.2
SO_3	5.6	1.7	2.0	2.3	2.5	2.8	3.1	3.4	3.7
K_2O	7.6	2.3	2.7	3.0	3.4	3.8	4.2	4.6	5.0
CaO	2.6	0.8	0.9	1.0	1.2	1.3	1.4	1.6	1.7
Cr_2O_3	1.6	0.5	0.6	0.6	0.7	0.8	0.9	1.0	1.0
MnO	0.5	0.2	0.2	0.2	0.2	0.3	0.3	0.3	0.3
Fe_2O_3	7.4	2.2	2.6	3.0	3.3	3.7	4.1	4.4	4.8
NiO	3.3	1.0	1.2	1.3	1.5	1.7	1.8	2.0	2.2
SrO	3.0	0.9	1.1	1.2	1.4	1.5	1.7	1.8	2.0
Cs_2O	5.0	1.5	1.8	2.0	2.3	2.5	2.8	3.0	3.3
Total	100.0	100.0	100.0	100.0	100.0	100.0	100.0	100.0	100.0
WL	100	30	35	40	45	50	55	60	65

The materials produced were examined with X-ray diffraction (XRD) using a DRON-4 diffractometer (Cu Kα radiation), scanning electron microscopy with energy dispersive spectrometry (SEM/EDS) using an a JSM 5610 LV + JED-2300 analytical unit, and infrared (IR) spectroscopy using a IKS-29 spectrophotometer (compaction of powdered materials in pellets with KBr). Chemical durability of the materials was determined using PCT procedure [7].

RESULTS AND DISCUSSION

As follows from XRD patterns the samples with waste loadings (WL) of up to 45 wt.% produced by quenching of melts onto a metal plate were found to be X-ray amorphous. At higher WLs the samples contained minor spinel structure phase and trace of nepheline. The slowly cooled (annealed) samples at up to 45 wt/% WLs were majorly amorphous but contained minor spinel structure phase and trace of nepheline (Fig. 1). At higher WLs nepheline became major phase. As follows from reference data, occurrence of nepheline offers negative effect on chemical durability of the glassy materials [8] because residual glass is depleted with Al_2O_3 and SiO_2. However this effect has been shown to be rather minor [9,10].

SEM/EDS data show that the annealed samples #4 is composed of major vitreous phase and minor spinel (Fig. 2 *a*). Chemical composition of the vitreous phase is rather constant over the bulk (Table II). Spinel forms two types of dendrite crystals. Crystals of the first generation spinel have submicron (nanoscale) size and their composition cannot be determined precisely. The second generation spinel forms individual crystals up to ~25 μm in size. Its composition is given in Table III.

The sample with 50 wt.% WL is composed of nepheline, spinel and residual vitreous phase (Fig. 2 *b-e*, Tables II and III). Chemical composition of the vitreous phase is rather constant over the bulk of the sample. The devitrification areas are composed of nepheline and interstitial glass and are occasionally observed as hexagonal metacrystals (Fig. 2 *b,c*). Nepheline forms isometric inclusions with indistinct crystallographic contours up to ~15 μm in size (Fig. 2 *d*). Its chemical composition (Table II) is recalculated well to formula with 4 oxygen ions (Table IV). The interstitials between the nepheline crystals are filled with residual glass. Spinel is represented by two generations. Spnel-1 forms submicron-sized isomeric crystals uniformly distributed over the bulk of the sample. Spinel-2 (Table III) forms individual cubic crystals up to ~10 μm in size (Fig. 2 *e*).

The sample at 55 w.% WL is nearly fully crystalline and also composed of nepheline, spinel, and interstitial glass (Fig. 2 *f,g* and Tables II and III). Moreover an extra aluminosilicate phase enriched with Cs_2O and depleted with Na_2O as compared to nepheline occurs (Fig. 2 *g* and Table II). Nepheline forms isomeric grains with a size of ~20 μm to 40-55 μm. The interstitials are filled with residual glass. Na-Cs aluminosilicate phase has light-gray color on SEM images in backscattered electrons (Fig. 2 *g*) and forms rather large elongated metacrystals. Spinel like in previous sample occurs as fine (first generation) and individual cubic (second generation) crystals.

The quenched sample at 60 wt.% WL is mainly amorphous but contains minor spinel forming fine (first generation) and larger (up to 5-10 μm in size) individual crystals distributed within the vitreous phase (Fig. 2 *h-j* and Table III).

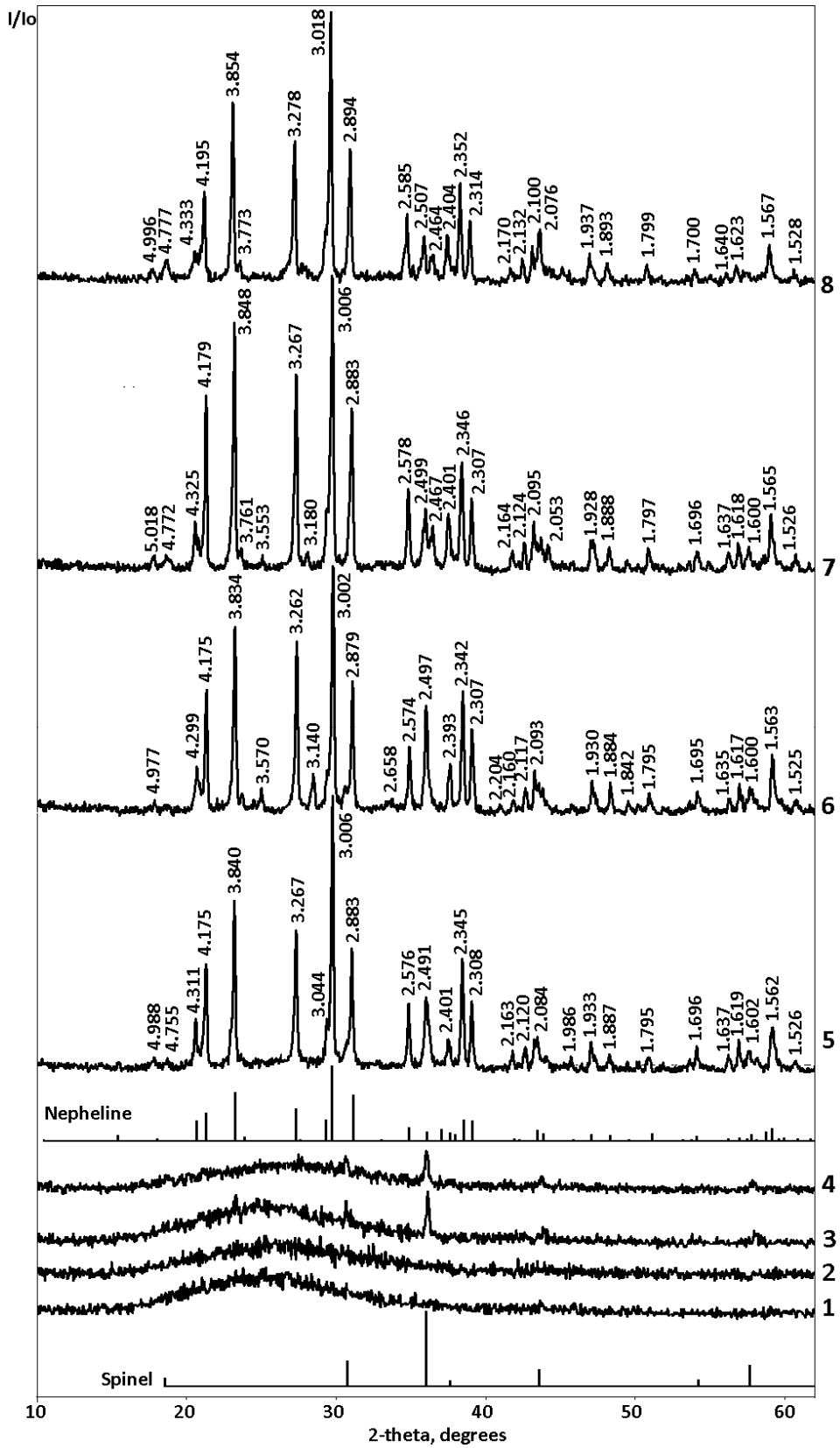

Fig. 1. XRD patterns of the annealed samples.

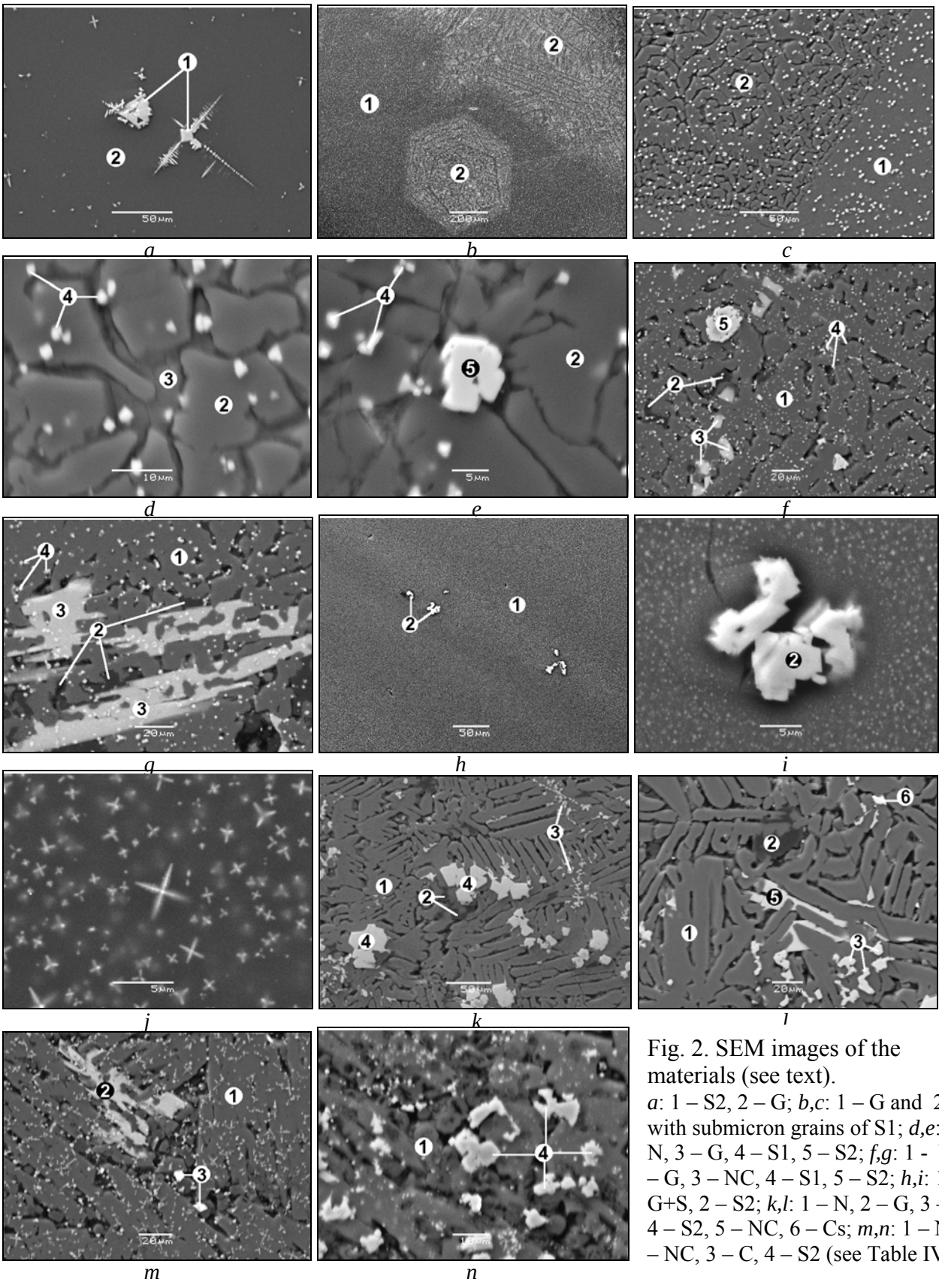

Fig. 2. SEM images of the materials (see text).
a: 1 – S2, 2 – G; *b,c*: 1 – G and 2 – N with submicron grains of S1; *d,e*: 2 – N, 3 – G, 4 – S1, 5 – S2; *f,g*: 1 - N, 2 – G, 3 – NC, 4 – S1, 5 – S2; *h,i*: 1 – G+S, 2 – S2; *k,l*: 1 – N, 2 – G, 3 – S1, 4 – S2, 5 – NC, 6 – Cs; *m,n*: 1 – N, 2 – NC, 3 – C, 4 – S2 (see Table IV).

Table II. Chemical composition (wt.%) of vitreous and aluminosilicate phases in the annealed samples.

Sample	4	5	6	7	5	6	7	8	6	7	8	7	8
Oxides	Vitreous phase				Nepheline				Na-Cs-Al silicate			Cs-Al silicate	
Li_2O	nd	nd.	nd	nd	-	-	-	-	-	-	-	-	-
B_2O_3	nd	nd	nd	nd	-	-	-	-	-	-	-	-	-
Na_2O	11.07	10.22	*0.38*	*0.46*	16.26	17.05	16.25	15.02	8.12	13.34	13.09	-	0.74
MgO	0.58	0.49	4.38	3.48	-	-	-	-	-	-	-	-	-
Al_2O_3	22.91	30.63	23.54	36.58	34.10	36.66	37.59	38.51	29.19	27.94	28.42	22.15	23.46
SiO_2	46.22	43.42	49.75	39.16	42.37	38.97	37.19	34.95	30.88	26.28	25.57	22.55	22.74
SO_3	0.52	-	-	-	-	-	-	-	3.33	4.94	5.66	-	-
K_2O	3.89	3.96	0.10	-	4.84	5.06	5.44	5.88	2.67	1.06	1.31	1.20	1.42
CaO	1.56	1.77	nd	nd	nd	nd	0.53	1.03	-	0.48	0.53	-	-
Cr_2O_3	0.60	-	nd	nd	-	-	-	-	3.06	0.99	-	0.22	0.23
MnO	*0.17*	-	nd	nd	-	-	-	-	-	-	-	-	-
Fe_2O_3	2.96	2.11	2.05	1.81	1.42	1.13	1.30	1.42	1.06	0.39	1.33	0.53	1.18
NiO	0.35	-	nd	nd	-	-	-	-	-	-	-	-	-
SrO	1.59	1.61	nd	*0.17*	*0.40*	0.58	1.17	2.37	-	1.41	1.43	-	-
Cs_2O	2.39	1.27	nd	-	0.60	0.55	0.53	0.82	21.69	23.17	22.66	53.34	50.23
Total	94.81	95.48	80.10	81.49	100.00	100.00	100.00	100.00	100.00	100.00	100.00	100.00	100.00

nd – not determined, "-" oxide concentration is <0.01.

Table III. Chemical compositions (wt.%) of spinel phases in the quenched (q) and annealed (a) samples.

Oxides	4a	5a	6a	7q	7a	8a
MgO	0.71	3.09	3.95	4.27	2.86	4.67
Al_2O_3	4.10	12.25	32.35	59.31	27.17	61.09
Cr_2O_3	29.59	46.65	23.53	4.01	9.09	1.87
MnO	0.93	1.29	0.98	0.63	0.89	0.73
Fe_2O_3	31.77	16.75	16.17	9.30	31.06	11.32
NiO	29.01	19.97	23.02	22.49	28.94	20.33
Total	96.11	100.00	100.00	100.00	100.00	100.00

The sample with the same composition but slowly cooled in turned-off furnace is fully crystalline and consists of nepheline, spinel, interstitial glass and two Cs-bearing aluminosilicate phases (Fig. 2 *k,l* and Tables II and III). Nepheline forms large elongated crystals. Cs is partitioned between mixed Na-Cs aluminosilicate and $CsAlSiO_4$. The Na-Cs aluminosilicate has light-gray color and is located in interstitials between the elongated nepheline crystals (Fig. 2 *l*). Cs analog of kalsilite forms individual grains white on SEM images (Fig. 2 *k,l*) few microns in size and has constant composition recalculated well to a formula with four oxygen ions. Spinel like in previous samples occurs as submicron (first generation) and micron-sized (second generation) crystals.

Table IV. Summary of formulae of crystalline phases in the samples.

Sample	Phase	Formula
4a	Spinel-2 (S2)	$Mg_{0.04}Mn_{0.03}Ni_{0.91}Fe_{0.92}Cr_{0.91}Al_{0.19}O_4$
5a	Spnel-2 (S2)	$Mg_{0.16}Mn_{0.04}Ni_{0.55}Fe_{0.43}Cr_{1.25}Al_{0.49}O_4$
	Nepheline (N)	$Na_{0.76}K_{0.15}Cs_{0.01}Sr_{0.01}Al_{0.97}Fe_{0.03}Si_{1.02}O_4$
6a	Spinel-2 (S2)	$Mg_{0.18}Mn_{0.03}Ni_{0.58}Fe_{0.38}Cr_{0.58}Al_{1.19}O_4$
	Nepheline (N)	$Na_{0.81}K_{0.16}Cs_{0.01}Sr_{0.01}Al_{1.05}Fe_{0.02}Si_{0.95}O_4$
	Na-Cs aluminosilicate (NC)	$Na_{0.45}K_{0.10}Cs_{0.26}Sr_{0.02}Al_{0.98}Fe_{0.02}Cr_{0.07}Si_{0.88}S_{0.07}O_4$
7q	Spinel-2 (S2)	$Mg_{0.18}Mn_{0.02}Ni_{0.51}Fe_{0.22}Cr_{0.09}Al_{1.96}O_4$
7a	Spinel-2 (S2)	$Mg_{0.14}Mn_{0.03}Ni_{0.76}Fe_{0.77}Cr_{0.24}Al_{1.05}O_4$
	Nepheline (N)	$Na_{0.77}K_{0.17}Cs_{0.01}Sr_{0.02}Al_{1.09}Fe_{0.02}Si_{0.91}O_4$
	Na-Cs aluminosilicate (NC)	$Na_{0.77}K_{0.04}Cs_{0.29}Ca_{0.02}Sr_{0.02}Al_{0.98}Fe_{0.01}Cr_{0.02}Si_{0.78}S_{0.11}O_4$
	Cs aluminosilicate (C)	$Cs_{0.94}K_{0.06}Al_{1.07}Fe_{0.02}Cr_{0.01}Si_{0.97}O_4$
8a	Spinel-2 (S2)	$Mg_{0.19}Mn_{0.02}Ni_{0.45}Fe_{0.23}Cr_{0.04}Al_{1.96}O_4$
	Nepheline (N)	$Na_{0.73}K_{0.19}Cs_{0.01}Ca_{0.03}Sr_{0.03}Al_{1.13}Fe_{0.03}Si_{0.87}O_4$
	Na-Cs aluminosilicate (NC)	$Na_{0.75}K_{0.05}Cs_{0.29}Ca_{0.02}Sr_{0.02}Al_{0.99}Fe_{0.03}Si_{0.76}S_{0.13}O_4$
	Cs aluminosilicate (C)	$Cs_{0.85}K_{0.07}Na_{0.06}Al_{1.10}Fe_{0.04}Cr_{0.01}Si_{0.90}O_4$

The sample at 65 wt.% WL is fully crystalline and composed of spinel, nepheline and Cs-bearing phases (Fig. 2 *m,n* and Tables II and III). Nepheline being major phase forms large isomeric gray crystals. Mixed Na-Cs aluminosilicate has light-gray color and fills interstitials between the nepheline crystals. Cs aluminosilicate forms white individual grains up to several microns in size. Spinel (second generation) forms regular cubic crystals up to 50 μm in size.

Chemical compositions of the phases are changed with compositions of glassy materials (waste to frit ratio). Composition of spinel-2 is being depleted with Fe and Ni and enriched with Al till up to formation of herzinite-type phase. Nepheline may incorporate K^+ ions in amount of up to 0.19 formula units (fu). Cs exhibits a tendency to formation of separate phases because nepheline has a low isomorphic capacity with respect to Cs^+ ions. Maximum Cs_2O concentration in nepheline reached ~0.8 wt.% or ~0.01 Cs fu. At higher Cs content the mixed Na-Cs aluminosilicate which may incorporate of up to ~23 w.% Cs_2O or 0.29 Cs fu occurs. This phase has the same chemical formulae as nepheline but different crystal structure providing for incorporation of higher Cs concentrations. Major features of this phase is anomalously high concentration of sulfate ions – up to ~5.7 wt.% SO_3 or 0.13 S fu. Sulfur incorporation as S^{6+} or SO_4^{2-} ions into crystal lattice may be facilitated in the presence of large Cs^+ cations. Simplified suggested formula of this phase may be represented as $Na_{0.8}Cs_{0.3}AlSi_{0.8}S_{0.1}O_{3.95}$. At high Cs content formation of Cs analog of nepheline or kalsilite with nominal formula $CsAlSiO_4$ occurs.

IR spectra of the materials shown on Fig. 3 consist of the same bands within the wavenumber ranges of 1500-1300 cm^{-1}, 1300-1250 cm^{-1}, 1200-800 cm^{-1}, 750-600 cm^{-1} and lower 600 cm^{-1}. Attribution of the band at 1500-1350 cm^{-1} normally observed in spectra of alkali-silicate glasses is uncertain. This band was associated with bending modes in metal hydroxides, structurally bound or absorbed water or stretching modes in CO_3^{2-} ions. In the spectra of borate and borosilicate glasses the wavenumber ranges of 1550-1300 cm^{-1} and ~1260-1270 cm^{-1} are typical of vibrations in the boron-oxygen groups with trigonally coordinated boron (boron-oxygen

triangles BO_3). These bands were attributed as components of twice degenerated asymmetric valence ν_3 O−B−O vibrations (stretching modes). The band with components ~710-730 and 650-670 cm^{-1} may be associated with twice degenerated asymmetric deformation δ (ν_4) O−B−O vibrations (bending modes) [11]. Strong absorption in both IR and Raman spectra within the range of 1150-850 cm^{-1} is caused by asymmetric ν_3 vibrations (stretching modes) in silicon-oxygen units being isolated (850-900 cm^{-1}) or bound to one (~900-950 cm^{-1}), two (~950-1050 cm^{-1}), three (~1050-1100 cm^{-1}) and four (~1100-1150 cm^{-1}) neighboring SiO_4 tetrahedra (Q^0, Q^1, Q^2, Q^3, Q^4, respectively) [12] and, in less extent, BO_4 tetrahedra (1000-1100 cm^{-1}) [13]. The bands due to bending modes in low-symmetry SiO_4 tetrahedra (Q^1, Q^2, Q^3) are positioned at 800-700 cm^{-1}. In IR spectra of all the glasses the broad band within the range of ~800-1200 cm^{-1} is multicomponent due to superposition of vibrations (stretching modes) in SiO_4 and BO_4 tetrahedra. Stretching modes of Al—O bonds in AlO_4 tetrahedra and Fe—O bonds in FeO_4 tetrahedra are positioned at 700-800 cm^{-1} and 550-650 cm^{-1}, respectively. Bending modes of Si—O—Si bonds in SiO_4 tetrahedra are positioned within the range of 350-550 cm^{-1}.

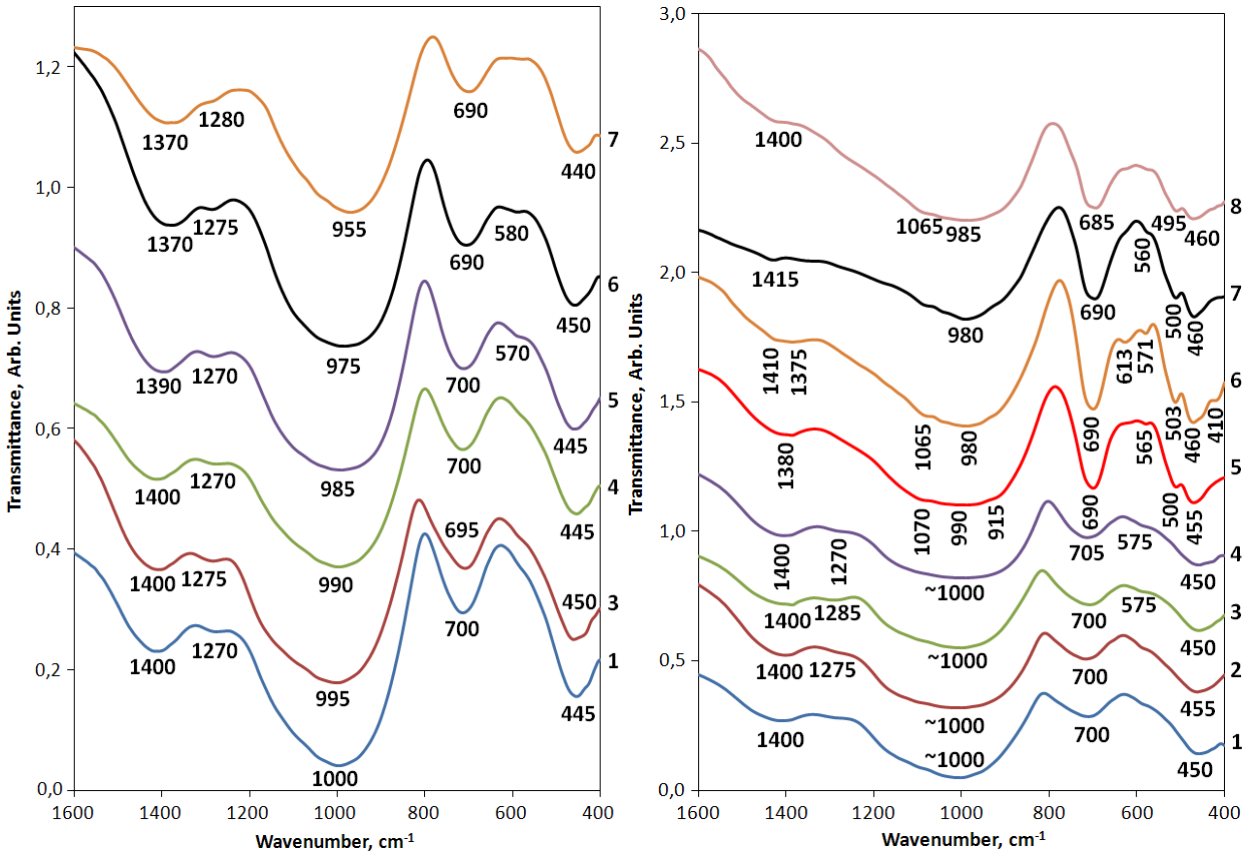

Fig. 3. IR spectra of the quenched (left) and annealed (right) materials within the range of 1600-400 cm^{-1}.

With the increase of WL the following changes in IR spectra of quenched samples occur: maximum of the band 1500-1300 cm^{-1} is shifted from 1400 cm^{-1} to 1370 cm^{-1}, the bands 1200-800 cm^{-1} and 750-600 cm^{-1} are reduced in intensity and their maxima are shifted from ~1000

cm^{-1} to ~ 955 cm^{-1} and from 700 cm^{-1} to 690 cm^{-1}, respectively, and a weak band at ~570-580 cm^{-1} arrears. The changes observed may be due to decrease of the degree of connectedness (polymerization) of silica-oxygen network because of decrease of silica content in the materials while increasing of alumina and, in much less extent, Fe_2O_3 content is unable to compensate the number of breaks in the silica-oxygen network by AlO_4 tetrahedra with bridging oxygens. As a result, fraction of SiO_4 tetrahedra with one bridging oxygen increases causing a shift of the maxima of the bands due to asymmetric and symmetric stretching modes in SiO_4 tetrahedra to lower wavenumbers. At the same time increase of Al_2O_3 content in the materials is responsible for formation of the band at 570-580 cm^{-1} due to sixfold-coordinated aluminum.

The IR spectra of the annealed materials are markedly influenced by occurrence of crystalline phases – spinel and alkali aluminosilicates. At relatively low WLs (30-45 wt.%) the spectra are similar to those of quenched samples. At higher WLs the bands at 1200-850 cm^{-1}, 700-600 cm^{-1} and lower 600 cm^{-1} in IR spectra become comparable on their intensities, the band at 1200-800 cm^{-1} broadens towards higher wavenumbers with formation of a component at ~1065 cm^{-1}, at lower 600 cm^{-1} additional bands appear. Increase of the number of the bands is normally due to segregation of crystalline phases. The bands positioned lower 600 cm^{-1} may be attributed as vibrations of Fe—O and Al—O bonds in spinels whereas additional bands within the ranges of 1200-800 cm^{-1} and 750-600 cm^{-1} may be assigned to the contribution of nepheline (~1085, 1045, ~1000, ~700, ~520 and ~480 cm^{-1} [14]). The bands due to B—O vibrations in BO_3 triangles (~1370-1400 cm^{-1} and ~1270-1285 cm^{-1}) decrease in intensity with the increase of WL till up to be negligible.

Measurements of elemental normalized releases (NR) showed an increase of NR of B, Li, Na and Si with the increase of WL (Table V). The NRs are the strongest for Li and B and their change is symbiotic, whereas NRs of Na and , particularly Si, are markedly lower.

Table V. NRs (g/L) of B, Li, Na and Si from the materials at various WLs.

Quenched samples					Annealed samples				
WL	B	Li	Na	Si	WL	B	Li	Na	Si
30	0.48	0.50	0.33	0.29	30	0.45	0.47	0.37	0.29
35	0.48	0.54	0.37	0.29	35	0.48	0.53	0.40	0.30
40	0.52	0.62	0.40	0.30	40	0.52	0.66	0.48	0.33
45	0.55	0.66	0.45	0.33	45	0.86	1.00	0.77	0.35
50	0.67	0.75	0.49	0.37	50	1.27	1.35	0.92	0.37
55	0.84	0.90	0.56	0.40	55	1.52	1.84	1.17	0.40
60	1.23	1.25	0.62	0.50	65	2.44	2.50	1.30	0.40
EA[15]	18.11	9.99	13.78	4.04	65 [10]	0.95	0.88	0,69	0.23

EA - Environmental Assessment Glass

For comparison data on NLs of the same elements from the material containing 65 wt.% Sludge Batch 4 (high-Fe/Al) Savannah River Site waste and produced in a 236 mm inner diameter cold crucible at SIA Radon in Russia are also given in Table V. Anyway, NRs of all the elements studies were found to be much lower than those of EA glass. Even at 65 wt.% WL the NR values remain by 8 to 15 times lower than those recommended by EPA.

CONCLUSIONS

The materials produced by melting of mixtures of HLW calcine surrogate and Li-Na-borosilicate frit followed by quenching onto a metal plate were found to be predominantly amorphous at WLs of 30 to 45 wt.% and contained trace of crystalline phases at higher WLs. The samples with the same composition but slowly cooled in turned-off furnace were fully amorphous at 30 wt.% and 35 wt.% WL, contained spinel at 40 and 45 wt.% WL and were predominantly crystalline at 50 wt.% WL and higher. At high WLs nepheline was major phase and spinel and two Cs-bearing aluminosilicates were minor phases. The phase of mixed Na/Cs aluminosilicate incorporate of up to ~23 w.% Cs_2O or 0.29 Cs formula units and up to ~5.7 wt.% SO_3 or 0.13 S formula units. Chemical composition of the second Cs-bearing aluminosilicate phase is close to $CsAlSiO_4$.

Increase of WL in the material leads to depolymerization of structural network in the quenched samples. In the annealed samples increase of WL results in crystallization of aluminosilicates as well yielding increasing of NRs of the elements – Li and B in more and Na and Si – in less extent. In any case elemental NRs remain lower than those from the EA glass.

REFERENCES

1. S.A. DMTRIEV, S.V. STEFANOVSKY, "Management of Radioactive Waste" (Russ., Moscow, D. Mendeleev University of Chemical Technology Publ., 2000).
2. E. TRONCHE, J. LACOMBE, A. LEDOUX, R. BOEN, C. LADIRAT, "Vitrification of HLLW Surrogate Solutions Containing Sulfate in a Direc-Induction Cold Crucible Melter," Waste Management 2009 Conf. March 1-5, 2009, Phoenix, AZ. CD-ROM. ID 9136.
3. V.V. LEBEDEV, D.Y. SUNTSOV, S.Y. SHVETSOV, S.V. STEFANOVSKY, A.P. KOBELEV, F.A. LIFANOV, S.A. DMITRIEV. "CCIM Technology for Treatment of LILW and HLW," Waste Management 2010 Conf., March 7-11, 2010, Phoenix, AZ. 2010, CD-ROM. ID 10209.
4. M. DELAUNAY, A. LEDOUX, J.-L. DUSSOSSOY, P. BOUSSIER, J. LACOMBE, C. GIROLD, C. VEYER, E. TCHEMITCHEFF, Vitrification of Savannah River Site HLW Sludge Simulants at CEA Marcoule Industrial-Scale Cold Crucible Induction Melter Demonstration Platform," Waste Management 2009 Conf. March 1-5, 2009, Phoenix, AZ. CD-ROM. ID 9186.
5. S.V. STEFANOVSKY, V.V. LEBEDEV, M.A. POLKANOV, D.Y. SUNTSOV, J.C. MARRA. Cold Crucible Vitrification and Characterization of Vitrified Savannah River Sludge Batch 4 Waste Surrogate // Waste Management 2010 Conf., March 7-11, 2010, Phoenix, AZ. 2010, CD-ROM. ID 10139.
6. Y.V. GLAGOLENKO, E.G. DROZHKO, S.I. ROVNY, *Radiation Safety Problems* (Russ.), [1] (2006) 23-34.
7. Standard Test Method for Determining Chemical Durability of Nuclear Waste Glasses: The Product Consistency Test (PCT). ASTM Standard C1285-94, ASTM, Philadelphia, PA (1994).

8. H. LI, P. HRMA, J.D. VIENNA, M. QIAN, Y. SU, D.E. SMITH, *J. Non-Cryst. Solids*, 331 (2003) 202 – 216.

9. S.V. STEFANOVSKY, A.P. KOBELEV, V.V. LEBEDEV, M.A. POLKANOV, D.Y. SUNTSOV, J.C. MARRA, "The Effect of Waste Loading on the Characteristics of Borosilicate SRS SB4 Waste Glasses," ICEM '09/DECOM '09: 12th International Conference on Environmental Remediation and Radioactive Waste Management. October 11-15, 2009, Liverpool, UK. CD-ROM (2009).

10. A.P. KOBELEV, S.V. STEFANOVSKY, V.V. LEBEDEV, M.A. POLKANOV, V.V. GORBUNOV, A.G. PTASHKIN, O.A. KNYAZEV, J.C. MARRA, "Cold Crucible Vitrification of SRS SB4 HLW Surrogate at High Waste Loadings," *Advances in Materials Science for Environmental and Nuclear Technology*. *Ceram. Trans*. **222** (2010) 91-104.

11. V.A. KOLESOVA, *Glass Phys. Chem.* (Russ.) **12** [10] (1986) 4-13.

12. V.N. ANFILOGOV, V.N. BYKOV, A.A. OSIPOV, "Silicate Melts," (Russ., Nauka, Moscow (2005).

13. I.I. PLUSNINA, "Infrared Spectra of Minerals", (MGU, Moscow, 1977).

14. I.I. PLUSNINA, "Infrared Spectra of Silicates", (MGU, Moscow, 1967).

15. J.R. HARBOUR, "Summary of Results for Macrobatch 3 Variability Study," WSRC-TR-2000-00351 (2000).